J. Fluid Mech. (1985), *vol.* 159, *pp.* 1–18
Printed in Great Britain

Evolution of a single wake behind a pair of bluff bodies

By C. H. K. WILLIAMSON†
Engineering Department, University of Cambridge

(Received 25 February 1983 and in revised form 1 April 1985)

In this paper the flow behind a pair of bluff bodies placed side by side in a stream is studied using a variety of flow-visualization methods. Above a critical gap size between the bodies, vortex-shedding synchronization occurs, either in phase or in antiphase. It has previously been assumed that such synchronization forms a wake comprising two parallel vortex streets in phase and in antiphase respectively. In the present paper we find that two antiphase streets are indeed formed, although in-phase shedding leads to the development of a single large-scale wake. The vortices which are formed simultaneously at the cylinders rotate around one another downstream, each pair forming a 'binary vortex'. The combined wake comprises a street of such vortices, which we term a binary vortex street. Below a critical gap size between the bluff bodies the flow becomes asymmetric. We observe in this regime certain harmonic modes of vortex shedding whereby the shedding frequency on one side of the wake is a multiple of that on the other. Again, a large-scale wake is formed downstream. The present observations lead to a new interpretation of hot-wire-frequency data from other studies in terms of the harmonic modes.

1. Introduction

Investigations of the fluid flow and vortex dynamics about simple configurations of bodies helps our understanding of the flows around more complex and larger-scale structures, for example the flow around neighbouring buildings. Many studies have been directed towards the case of steady flow past groups of cylinders. Zdravkovich (1977*a*, *b*) has reviewed the problem of mutual interference between pairs of cylinders in a steady flow. He made particular reference to the side-by-side and in-line arrangements of the cylinder pair. Previous studies with the side-by-side configuration have involved measurements of force, pressure distribution and vortex frequency, as well as flow visualization. A brief review of the previous work is set out below.

When the gaps between cylinders are in range $1.0 < g^* < 5.0$, where g^* is the gap between cylinder surfaces/diameter, vortex-shedding synchronization (both in phase and in antiphase) has been found. Previously reported wake configurations are shown in idealized form in figure 1, where we note that antiphase vortex shedding occurs when each cylinder synchronously forms vortices of opposite sign. Landweber (1942) found that the vortex shedding was mainly in phase, Thomas & Kraus (1964) observed it to synchronize either in phase or in antiphase, and more recent studies have shown a predominance of antiphase shedding (Ishigai *et al.* 1972; Bearman & Wadcock 1973; Quadflieg 1977).

When the gaps between cylinders are smaller than $g^* = 1.0$, the wakes behind each cylinder become distinctly different. The vortex-shedding frequencies on one cylinder

† Present address: Graduate Aeronautical Labs, CALTECH, Pasadena, CA91125, USA.

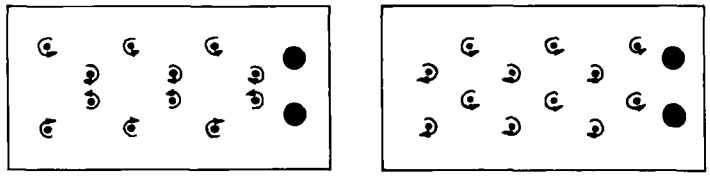

(a) Antiphase (b) In phase

FIGURE 1. Idealized vortex configurations in the wake of a pair of bluff bodies normal to a stream. (a) Two parallel streets in antiphase from antiphase vortex shedding. (b) Two parallel streets in phase from in-phase vortex shedding. Cylinders translating from left to right.

are markedly higher than for the other cylinder (for example see Spivack 1946). The gap flow becomes stably deflected to the high-frequency side of the wake, and the cylinder on this side experiences a greater drag force than the other cylinder. There exists a mean repulsive lift force between the cylinders. The structure of the near wake has been previously shown from flow visualization to be confused in this 'asymmetric-flow regime', and very little has been deduced about the form of the wake flow. However, the deflection of the gap flow has been demonstrated (Ishigai *et al.*, Bearman & Wadcock, Quadflieg) for Reynolds number in the region of 10^4 or above.

The total cylinder-pair drag force increases as gaps are reduced from $g^* = 4.0$ to 1.0. For smaller gaps the combined drag can become less than twice the isolated-cylinder drag (for example, Bierrman & Herrnstein 1933; Quadflieg).

The present paper mainly involves flow visualization behind a pair of circular cylinders, and also behind a pair of flat plates normal to a steady stream. Dye- and smoke-visualization techniques are used. Where antiphase-vortex-shedding synchronization occurs the visualization in §3 clearly demonstrates that the resulting wake is a pair of antiphase parallel streets as found in other studies. However, in-phase shedding at the cylinders does not lead to two in-phase parallel streets as previously supposed, but rather to a large-scale combined wake. The like-signed vortices pair up and a 'binary-vortex' street is formed. Flow visualization in §4 also shows that, when the bodies are sufficiently close to produce an asymmetric wake, there is a distinct mode of shedding when the vortex-shedding frequency on one side of the wake is a multiple of that on the other side. Such a harmonic mode of vortex shedding has hitherto not been suggested.

2. Experimental methods

The present study of the vortex wakes of two bodies involves flow visualization using both smoke in a wind tunnel and dye in a water channel. For the smoke visualization a vertical low-speed wind tunnel with upward flow is used, which has a working section 12×6 in. in cross-section, and is 20 in. long. Two side-by-side cylinders of external diameter 0.043 in. spanning the shortest dimension of the working section were used to generate the vortex wakes. We assume blockage is negligible because the ratio of the channel width to cylinder diameter is 280:1. The 'smoke' is actually liquid kerosene in the form of fine droplets formed in a smoke generator of the Preston & Sweeting (1943) type. Reynolds numbers were in the range 50–150. A Nikon camera is used in both methods of visualization (with 1 ms exposure times when using smoke). The smoke is illuminated by two 1000 W halogen bulbs providing a slit of light halfway along the length of the cylinders.

For the dye visualization a closed-circuit water channel is used of depth 10 cm with

a special pump which can drive a very weak density-stratified flow, while causing a minimum of vertical mixing. The pump consists of two counter-rotating stacks of intermeshing Perspex disks which are turned by an electric motor, the speed of which is controlled by varying the supply voltage. The fluid is driven through an observation section in the return leg of the channel 80 cm long by 10×10 cm cross-section. Pairs of cylinders (diameter 0.8 cm) and pairs of flat plates (width 0.8 cm) are used in the channel, giving a Reynolds number of around 200. The top half-volume of the fluid in the channel is mainly water (of density ρ_2), and the lower half-volume is weak salt solution (of density ρ_1). The ratio of the density difference divided by the mean density (between the two half-volumes) is around 0.01. The purpose of using this channel is that a dye with a mean density $\frac{1}{2}(\rho_1+\rho_2)$ will float roughly halfway up the channel at a constant horizontal level, thus providing clear flow visualization of the vortices. Observations of the flow showed that even with the effects of blockage (channel width : diameter is 12 : 1), and the weak stratification, the main wake patterns were similar in the channel and in the wind tunnel. Photography is from above the channel, and light is produced with a 1000 W Halogen lamp.

3. Synchronized vortex shedding

Flow visualization described in the present paper indicates a predominance of antiphase vortex shedding between two side-by-side cylinders for gaps in the range $1.0 < g^* < 5.0$, giving a wake comprising two antiphase parallel streets (see figure 1 *a*). This vortex configuration may be seen in figure 2 using smoke in the wind tunnel at a Reynolds number Re of 100. The configuration is stable in that it keeps its form for large distances downstream as shown in (*a*) for $g^* = 5.0$, and in (*b*) for $g^* = 3.0$. Figure 3 demonstrates the antiphase streets using dye at $Re = 200$. Although antiphase shedding is predominant over the range $1.0 < g^* < 5.0$, it is possible for the flow to 'flip' to in-phase-shedding synchronization and *vice versa*. In general either mode continues for a large number of cycles. The antiphase wake represented by the configuration in figure 1 (*a*) has been found in a region close behind the cylinders in previous studies using other forms of visualization.

It has previously been assumed, however, that the in-phase vortex shedding also leads to an idealized wake configuration; in this case two in-phase streets in figure 1 (*b*). Rather than the idealized wake we find the development of a large-scale single wake in the following manner. We observe in the smoke tunnel in figure 4 (*a*) for $g^* = 3.0$ that the like-signed vortices (which are shed synchronously) pair up and rotate around one another. A sketch is drawn in figure 4 (*b*) from the photograph to clarify the pairing process. The dashed curves mark the smoke outline from the upper cylinder whilst the full curves correspond to the lower cylinder. Clockwise vortices marked on the sketch demonstrate the pairing phenomenon as the wake progresses downstream.

The pairing process leads to the evolution of a large-scale combined wake. In the present paper we define a binary vortex as a pair of like-signed vortices which rotate around one another,† to distinguish from a normal vortex pair which consists of two contra-rotating vortices (see Lamb 1932). Two rows of these binary vortices in a

† McGraw-Hill *Dictionary of Science and Technology Terms* (1978) 'Binary system: any system containing two principal components'. For example, a binary star is a binary system in which two stars revolve about their common centre of gravity.

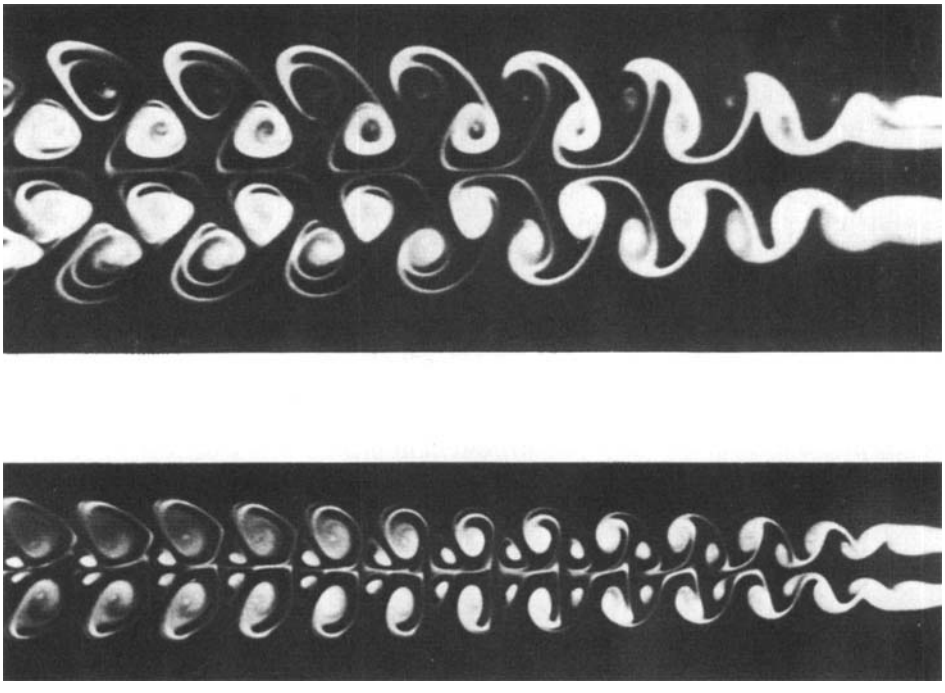

FIGURE 2. Antiphase synchronization of vortex shedding leading to two antiphase streets. Smoke visualization in the wind tunnel, flow from right to left. This 'idealized' vortex configuration is experimentally 'stable' in that it keeps its form for large distances downstream. $Re \approx 100$: (*a*) $g^* = 5.0$; (*b*) 3.0. The visualization in (*a*) is a larger scale than in (*b*).

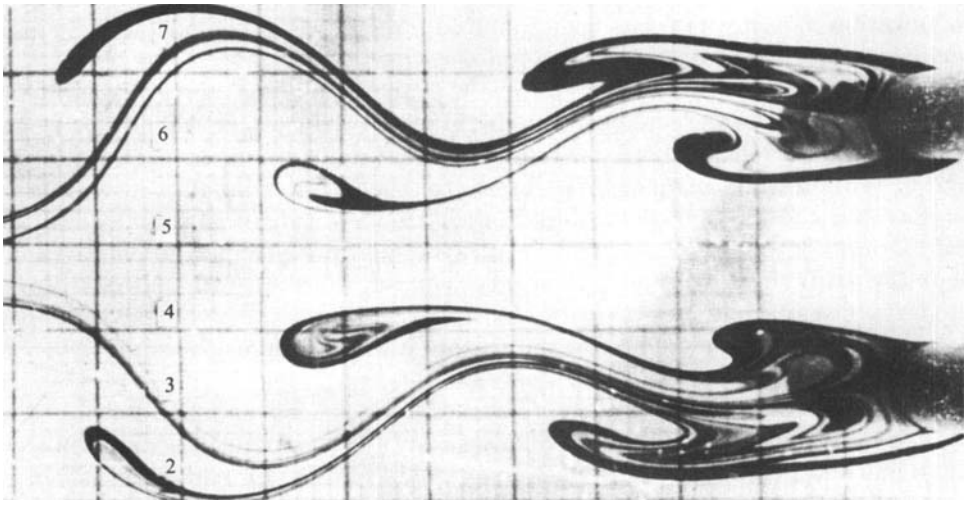

FIGURE 3. Antiphase vortex shedding. Dye visualization in the circulating-water channel, flow from right to left, $Re = 200$, $g^* = 2.0$.

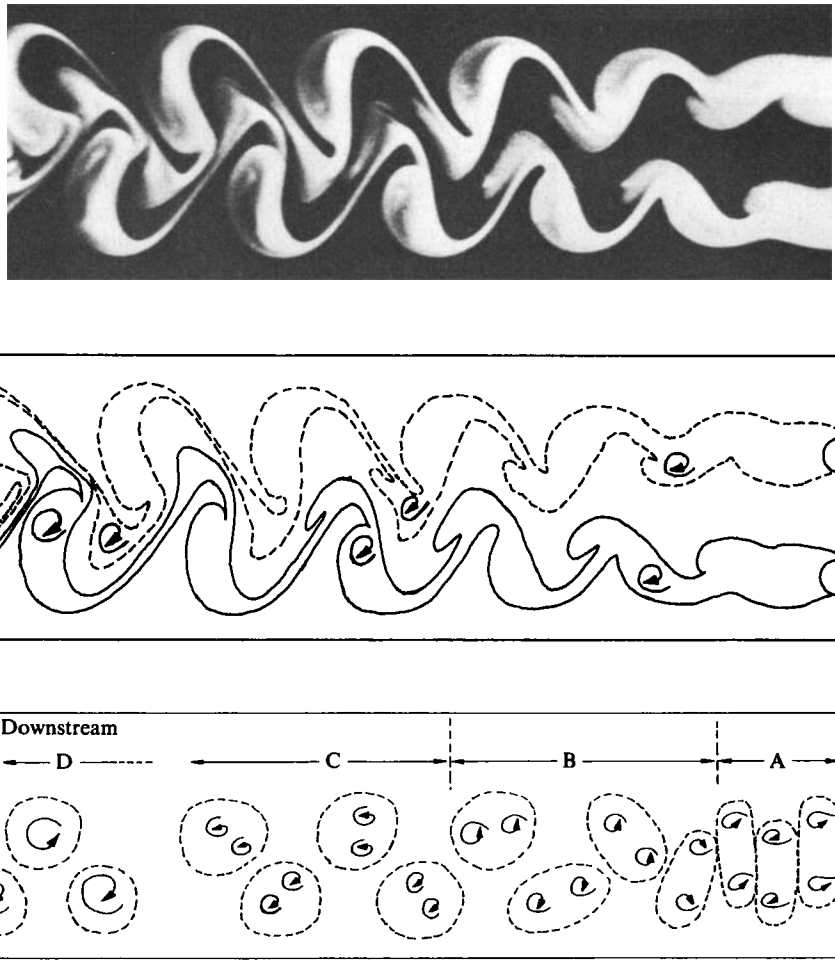

FIGURE 4. In-phase vortex shedding leading to the evolution of a binary street. (*a*) Smoke visualization in the wind tunnel, flow is from right to left, $Re = 100$, $g^* = 3.0$. The idealized configuration of figure 1 (*b*) is not 'stable' in that it cannot keep its form as the wake travels downstream, unlike the antiphase configuration. (*b*) Sketch of the visualization in (*a*) demonstrating the pairing up of like-signed vortices as the wake progresses downstream. Dotted curves are the smoke outlines from the upper cylinder, while full curves mark the smoke outlines from the lower cylinder. (*c*) Schematic development of a binary-vortex street. Region A close to the cylinder resembles the idealized vortex configuration of figure 1 (*b*). Region B: transition from two parallel wakes to a binary street. Region C: binary-vortex street. Region D: further downstream we may conjecture that each binary vortex coalesces to form a large-scale single street.

staggered arrangement (similar to the arrangement of single vortices in a Kármán street) is defined here as a binary-vortex street.

A diagram of the various flow regions downstream of the cylinders during the evolution of a binary-vortex street is shown in figure 4 (*c*). In region A, close to the cylinders, the vortex configuration resembles the idealized form of figure 1 (*b*), which is two parallel in-phase streets. Region B is a transition region as the two separate wakes of region A develop into the combined binary street found in Region C. We may conjecture that for some region downstream each binary vortex will coalesce into a single vortex, thus forming a large-scale Kármán street represented by

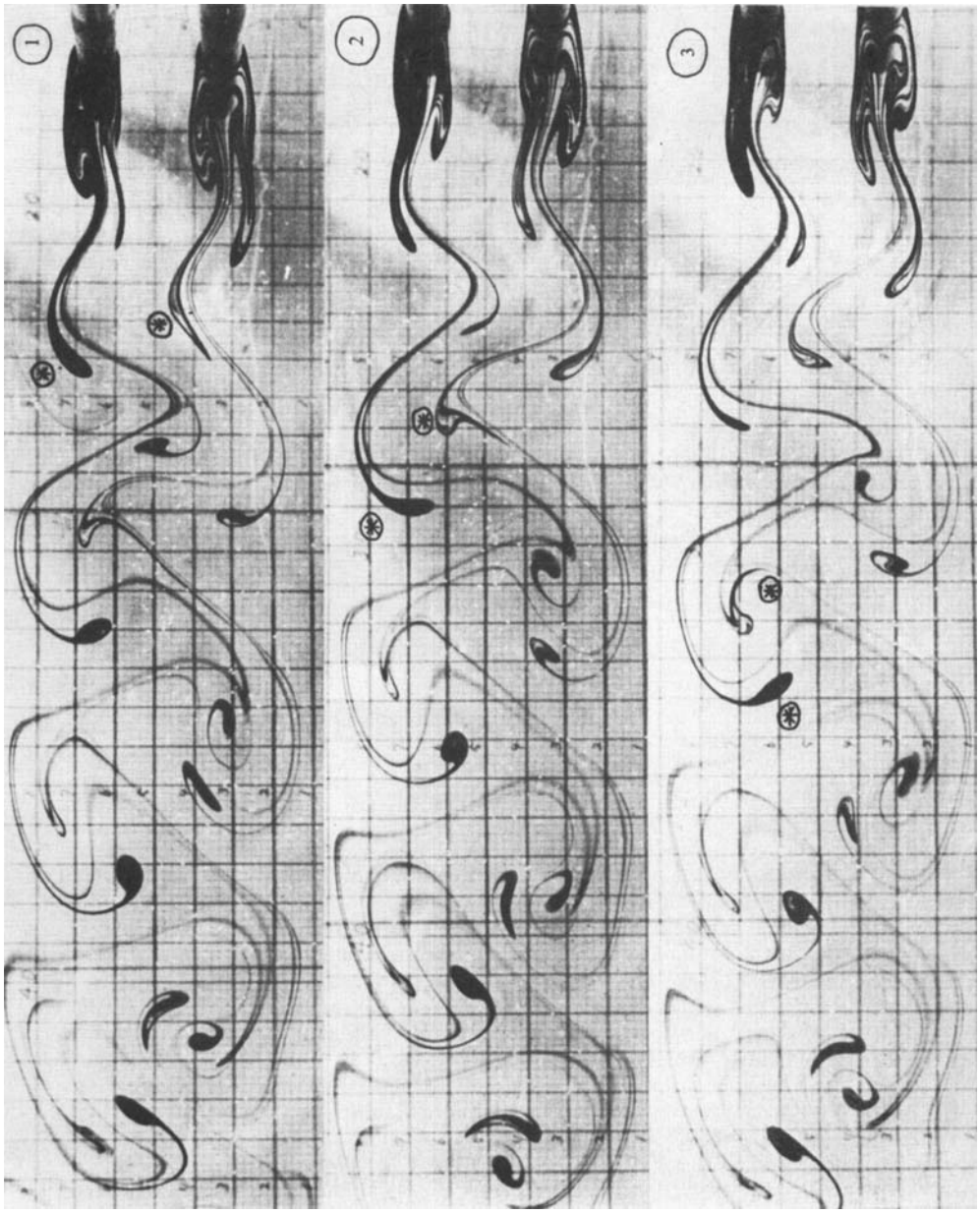

FIGURE 5. Binary-vortex street forming in the wake of two cylinders following in-phase vortex shedding. Dye visualization in the circulating-water channel, flow is from right to left, $Re = 200$, $g^* = 2.0$. Sequential photographs show vortices marked with asterisks forming a binary vortex.

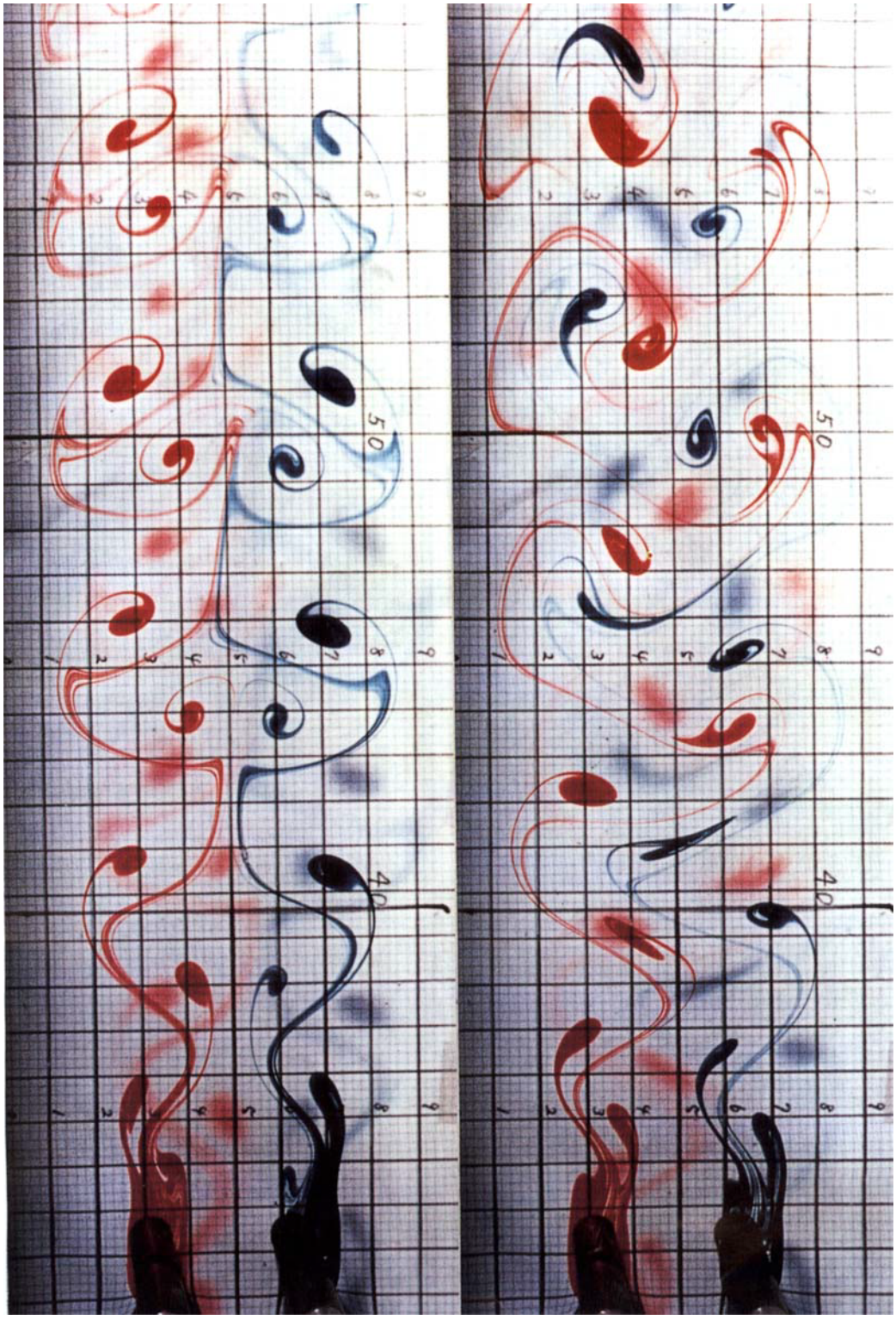

(a) *(b)*

FIGURE 6. Vortex-shedding modes and the formation of binary vortices. (Re = 200; g^*=2.4). *(a)* Antiphase parallel vortex streets formed from antiphase vortex shedding at the cylinders. *(b)* Binary vortex street formed from in-phase vortex shedding. Each binary vortex is composed of one red vortex from the left-hand cylinder and one blue vortex from the right-hand cylinder.

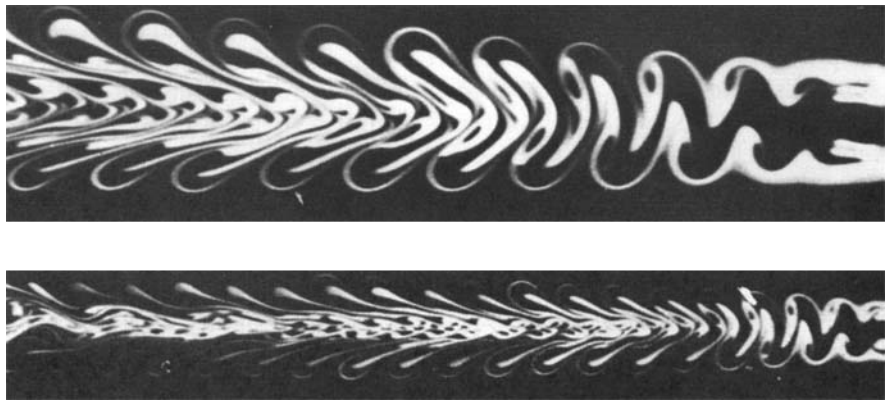

FIGURE 7. In-phase vortex shedding at the cylinders. Smoke visualization in the wind tunnel, flow is from right to left, $Re = 100$, $g^* = 3.0$. (*a*) and (*b*) show the smoke flowing round the outside edges of the cylinders, demonstrating fluid crossing from one side of the wake to the other. In (*b*), which is a smaller scale than (*a*), a sinuous oscillation of the wake develops far downstream.

region D. The length of region A increases as the gap is increased between the cylinders because the strength of the interaction between the two parallel wakes then diminishes. The vortex shedding 'locks' into the binary-street configuration mainly in the range $2.0 < g^* < 4.0$.

In figure 5 the binary-vortex street is demonstrated using dye for $g^* = 2.0$ and $Re = 200$. A typical binary vortex, marked with asterisks, is shown developing as the wake moves downstream in the sequential photographs.

A clear demonstration of both the wakes described above is found in figure 6 (plate 1). Here, in (*a*) and (*b*), the red vortices are formed behind the left cylinder and the blue vortices behind the right cylinder. There is little crossing over of one coloured dye to the other side of the wake in the antiphase pattern in (*a*). However the red and blue vortices in (*b*) from the gap rapidly cross over sides to form the binary vortices, each of which comprises one red and one blue vortex. The binary-vortex street of (*b*) is similar to the vortex street that may be visualized behind a single cylinder except that instead of two rows of single vortices we have two rows of binary vortices.

It should be noted that the dye and smoke filaments shown here represent streaklines which contain flow information integrated right back to the point at which the dye or smoke is introduced into the flow. For this reason some care should be taken in interpreting such streakline visualization far from its point of introduction. This has been pointed out recently by Cimbala (1984) who introduced smoke into the flow at various downstream positions behind a circular cylinder. Another characteristic of such visualization is that, at the low values of Reynolds numbers used in the present experiments, the vorticity diffuses more rapidly than the dye or the particular form of smoke used here. Although the dye, which originates from the cylinder surfaces, must indicate the position of the vortex sheets, the sheets themselves will be thicker than is indicated by the dye traces. The possible amalgamation of each binary vortex downstream into single large-scale vortices may thus occur sooner than suggested by the motion of the dye.

Finally, in figure 7 the smoke filaments are passed round the outside edges of the cylinders and show how fluid initially on one side of the wake finds its way rapidly

to the other side. The elongation of the smoke lines on the outside edges of the wake is caused by the relative upstream movement of the more central parts of the wake. Another phenomenon of interest is the developing sinuous oscillation of the complete wake some distance downstream of the cylinder pair in (*b*), which was also observed in the wake of a triangular array of three cylinders by Zdravkovich (1968). It has been shown by Cimbala that wake-velocity fluctuations due to the Kármán street behind a single cylinder decay rapidly with downstream distance. The identities of the individual vortices downstream become increasingly difficult to measure or to visualize when smoke is introduced downstream. However, as the wake is widening, a larger-scale structure emerges. Cimbala deduced that the larger wake oscillations were the result of the hydrodynamic instability of the developing mean-wake profile, and this may also explain the present large-scale oscillation in the downstream wake of a pair of cylinders following in-phase vortex shedding.

The present observations have been made for low Reynolds numbers of 100–200. However, observations and measurements in a region close behind a pair of cylinders at higher Reynolds numbers have demonstrated that vortices shed both in phase and in antiphase across the pair (for example Landweber 1942 at $Re = 1.3 \times 10^3$; Kamemoto 1976 at $Re = 662$; Quadflieg 1977 at $Re = 4 \times 10^4$). In conclusion, it seems likely that the binary-street wake observed in the present paper will also be in evidence when the vortex shedding is in phase at higher Reynolds numbers.

In the following section the cylinder gaps are reduced so that the wake becomes asymmetric. Using the visualization methods employed above we can show that even for smaller cylinder gaps there exist certain modes of vortex shedding.

4. Harmonic vortex shedding in the asymmetric-flow region

4.1. *Introduction*

In this section we describe the results of a flow-visualization study on the wake of two cylinders side by side in a steady flow when the vortex wake becomes distinctly asymmetric. This asymmetric-flow regime occurs in the present paper for gaps below about $g^* = 1.0$ for two cylinders, and below $g^* = 1.5$ for two flat plates. A brief survey of previous studies associated with the asymmetric-flow regime follows.

Landweber (1942) described the vortex shedding as confused between $g^* = 0.1$–1.0. Spivack (1946) measured the velocity-fluctuation frequencies using a hot-wire probe at a large number of points in the cylinder-pair wake. He found that behind one cylinder the frequencies were greater than behind the other when $g^* < 1.0$. He also noted that frequencies that were double the lower frequency appeared in certain positions in the flow, which he could not explain. For very low gaps ($g^* < 0.3$) he found that the vortex frequency was close to that associated with a solid body with the dimensions of the cylinder pair.

Ishigai *et al.* (1972), using schlieren visualization techniques (for $Re \approx 4 \times 10^3$) on cylinder pairs at various gaps and stagger angles, showed that the higher frequencies are measured on the side of the wake to which the gap flow deflects. The deflected gap flow was found to be bistable for the side-by-side case in that it remained deflected to one or the other side of the wake for long periods.

Simultaneous measurements on both cylinders of pressures and hence forces were subsequently undertaken. It has been found (Bearman & Wadcock 1973; Quadflieg 1977) that the high-frequency/thin-wake cylinder had a lower base pressure and higher drag coefficient, and also that the cylinders were pushed apart by a mean repulsive lift force.

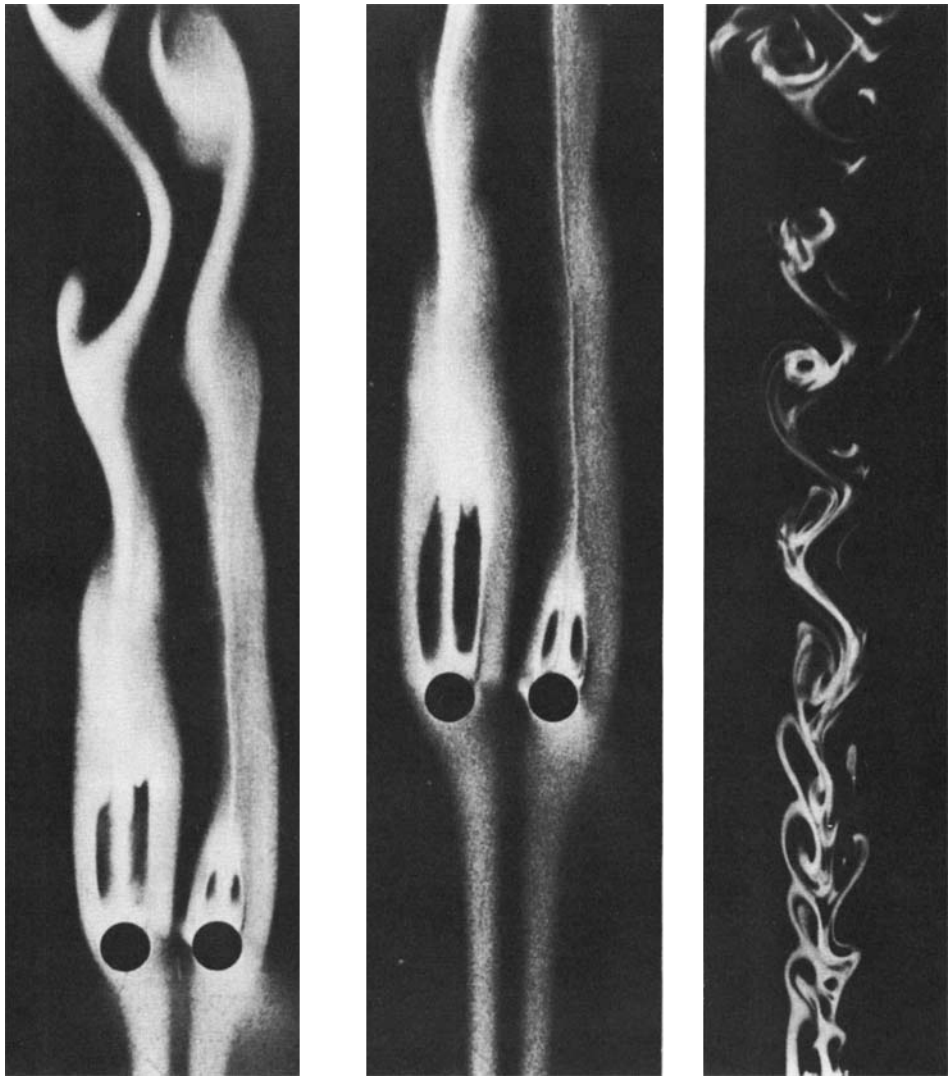

(*a*) (*b*) (*c*)

FIGURE 8. The wakes of a pair of cylinders in the 'asymmetric-flow region'. Smoke visualization in the wind tunnel, flow upwards. (*a*) and (*b*) show a bistable configuration of vortex pairs close to the cylinders, $Re = 55$, $g^* = 1.0$. The gap flow is deflected even at these low Reynolds numbers, and the wake vortex pairs have distinctly different sizes. (*a*) Shows a vortex wake developing downstream of the vortex pairs. (*c*) Shows the large-scale street wake behind a pair of cylinders, $Re = 100$, $g^* = 1.0$.

The flow asymmetry associated with a cylinder pair at small gaps is also a feature for larger numbers of cylinders arranged side by side in a steady flow. Measurements of drag force on rows of 3 and 4 cylinders by Gerhardt & Kramer (1981) suggest the existence of stably deflected gap flows, although this has not been shown. Roberts (1962) has found gap-flow asymmetry for a grid of cylinders arranged perpendicular to a flow.

In the case of the cylinder pair, flow visualization has shown the deflection of the

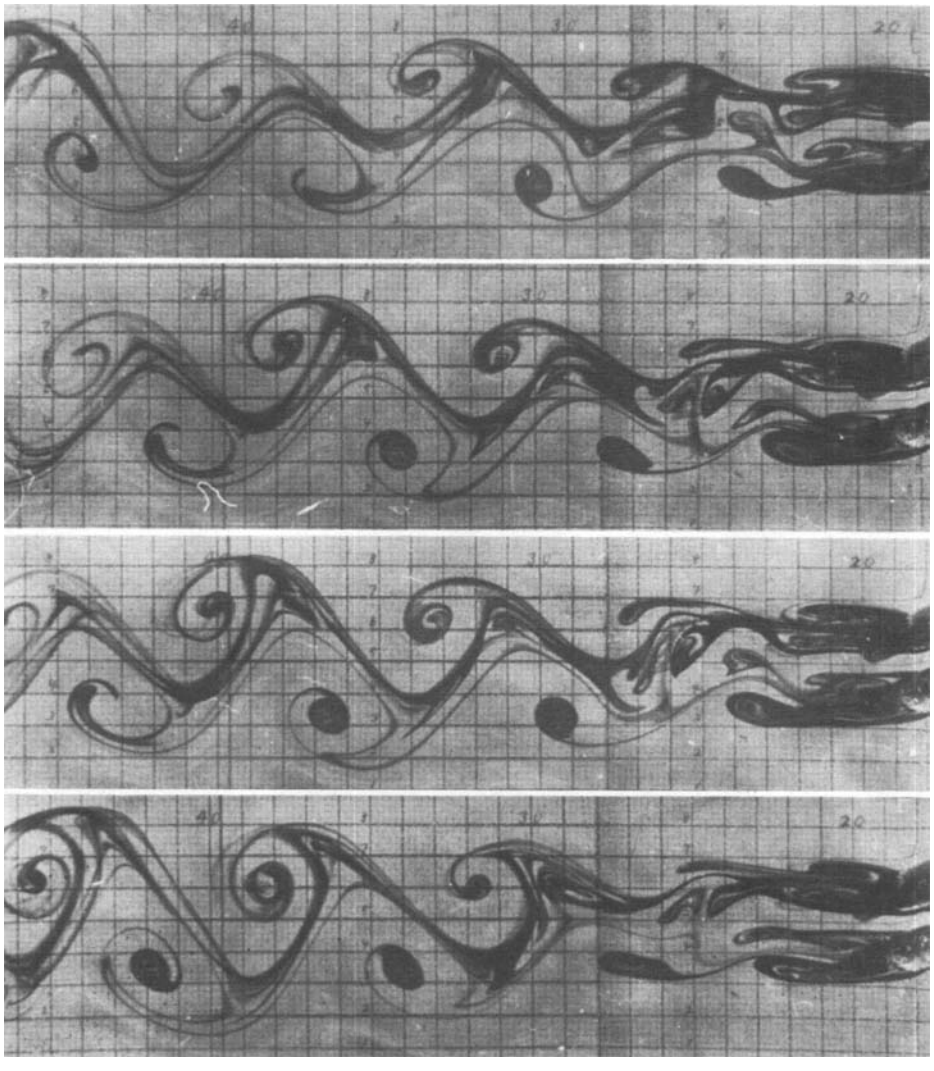

FIGURE 9. Fundamental mode of vortex shedding from two circular cylinders. Dye visualization in the water channel, flow is from right to left, $Re = 200$, $g^* = 0.85$.

gap flow (Ishigai *et al.*; Bearman & Wadcock; Quadflieg). However, previous visualization of the near wake has otherwise indicated rather confused flow.

In this section, we aim to throw new light on the vortex dynamics of the near wake in the asymmetric-flow regime. Distinct vortex-shedding modes are revealed for pairs of cylinders, and pairs of plates, which lead us to reinterpret the many frequency measurements in the wake of cylinder pairs from other investigations.

Finally, we observe briefly the deflected flows behind a three-cylinder row, and demonstrate the formation of a large-scale street downstream of the three cylinders.

4.2. *Vortex dynamics in the asymmetric-flow regime*

Visualization of certain modes of vortex shedding are made in the wake of two cylinders and two plates. Smoke filaments in a wind tunnel at $Re \approx 100$, and dye in

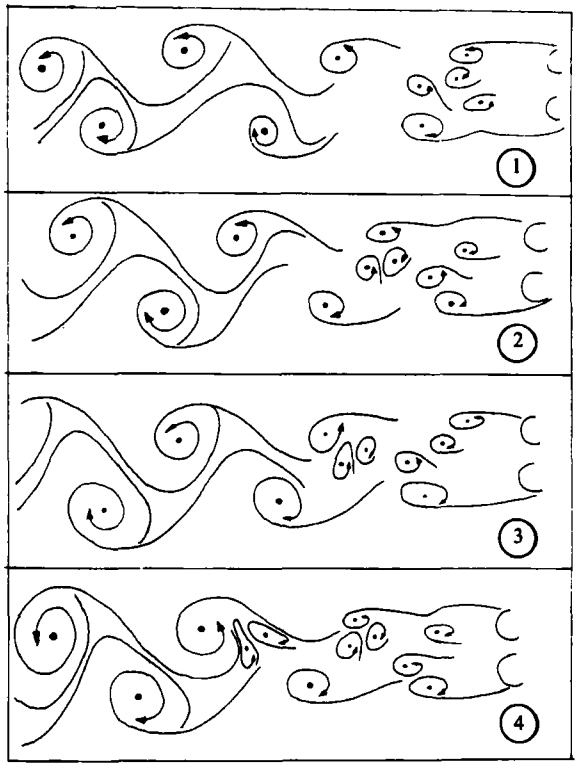

FIGURE 10. Schematic diagram of the fundamental mode of vortex shedding shown in figure 9. Vortex pairs from the gap are squeezed and amalgamated with dominant outer vortices, and this process occurs predominantly to one or the other side of the wake.

a circulating-water channel at $Re = 200$ are used to produce closely two-dimensional flow.

At very low Reynolds numbers ($Re = 55$) in the wind tunnel we observe the existence of wake vortex pairs or circulating regions behind each cylinder, as shown in figure 8. The significance of these vortex pairs compared with those normally found behind a single cylinder at low Reynolds numbers is that the length of the vortex pair behind one cylinder is around three times the length of the vortex pair behind the neighbouring cylinder. As a result we show that the gap flow is deflected to one side of the wake even for these low Reynolds numbers. The deflection is to the side with the smaller vortices. This configuration, as shown in figure 8, is experimentally stable in that it may be observed for long periods of time. Vortex-wake formation occurs from the rear end of the wake eddies. A large-scale street is shown downstream in figure 8(*c*) for $Re = 100$.

The most significant result of the flow visualization in the channel is the observation of certain harmonic modes of vortex shedding from the cylinder pair for $g^* < 1.0$. On one cylinder the frequency of the outer-surface vortex shedding is a multiple of that on the other cylinder and the lower controlling frequency is termed here the fundamental frequency. Visualization of the fundamental shedding mode is shown in figure 9. In this mode a large-scale Kármán street is soon formed downstream of the cylinders. A flow diagram of the vortex interaction in figure 10 demonstrates how pairs of 'gap vortices' from both cylinders are 'squeezed',

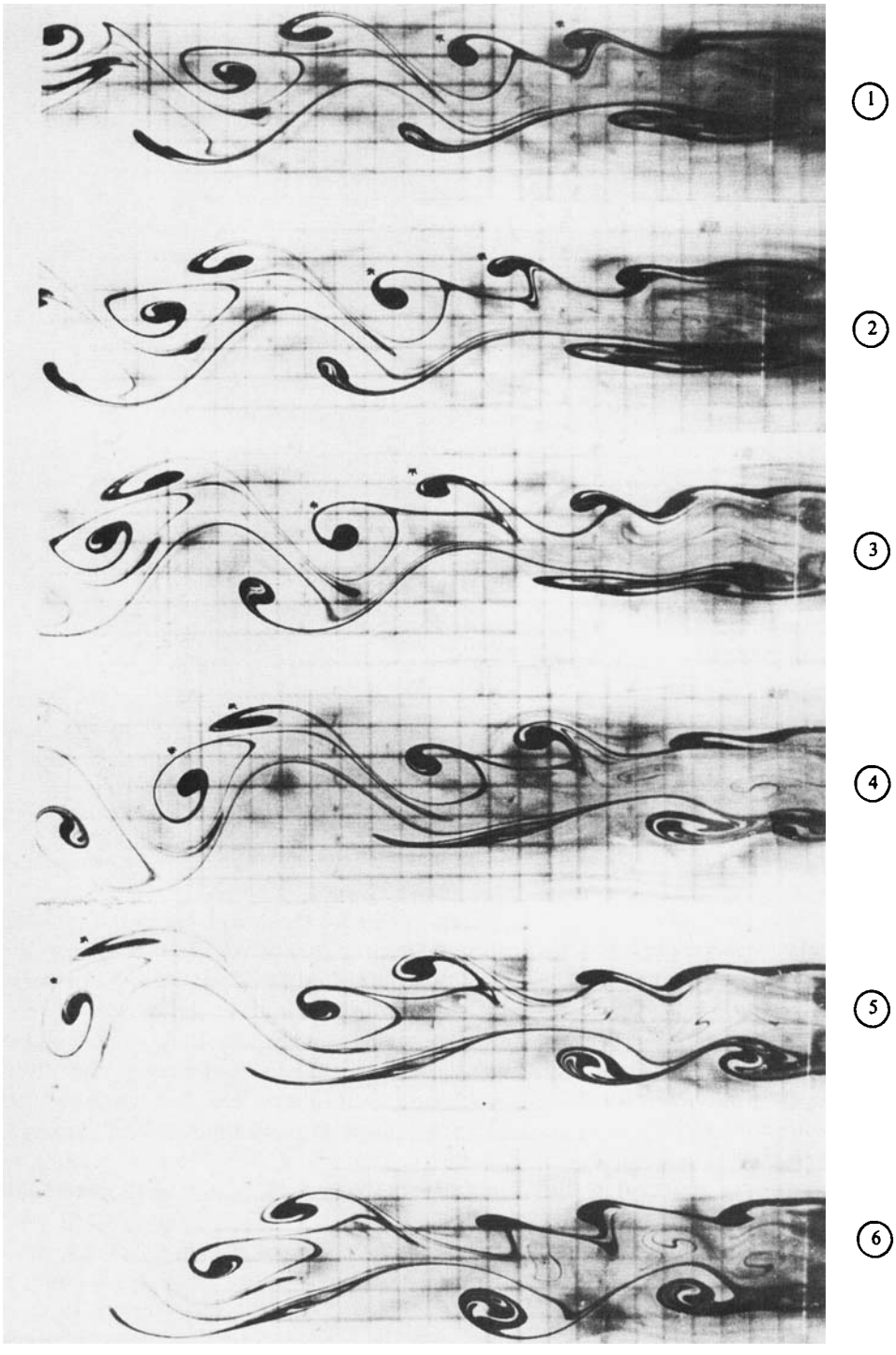

FIGURE 11. Second harmonic mode of vortex shedding from two circular cylinders. Dye visualization in the water channel, flow is from right to left, $Re = 200$, $g^* = 0.7$. Vortices marked with asterisks are seen to pair up on the upper side of the wake in the sequential photographs.

FIGURE 12. Second harmonic mode of vortex shedding from two flat plates. Dye visualization in the water channel, flow is from right to left, $Re = 200$, $g^* = 1.0$. In this case the gap flow is deflected to the lower side of the wake.

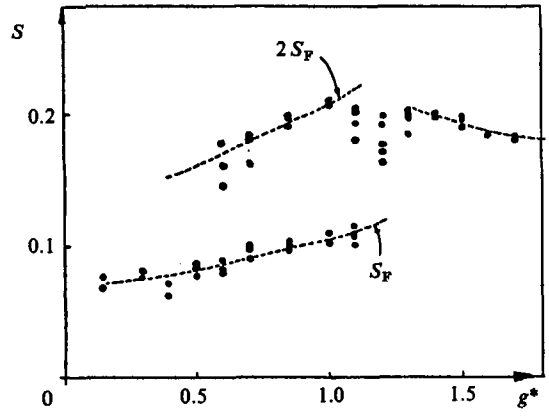

FIGURE 13. Vortex-shedding frequency for two flat plates side by side in a stream. From the water channel, using dye visualization, $Re = 200$.

weakened and amalgamated with dominant outer vortices. This occurs predominantly to one side of the wake, and in this example the gap flow is weakly deflected upwards.

The second harmonic mode of vortex shedding is shown in figure 11. In this mode the near wake consists of pairs of vortices on one side of the wake and single large vortices on the other side. The gap flow deflects to the higher-frequency side of the wake (this is upwards in figure 11). The photographs in figure 11 are sequential and typical flow development may be followed by referring to the pair of vortices marked with asterisks. The frequency of the gap vortices that shed as pairs is the same as the frequency of the outer vortices on the thin-wake side (to which the gap flow deflects). In this mode, as in the fundamental mode, the inner vortex pairs are squeezed, distorted and amalgamated with the dominant outer vortices on the thin-wake side. This flow pattern occurs roughly in the range $g^* = 0.6$–0.9 for cylinder pairs.

Although we have observed mainly a second harmonic mode in the asymmetric-flow regime, smaller periods of time were found when a pair of vortices was followed by a weak third vortex. This constitutes a third harmonic mode. However, the main mode at these low Reynolds numbers is found to be the second harmonic. The second harmonic mode is also found to be intermittent. In such periods when this mode

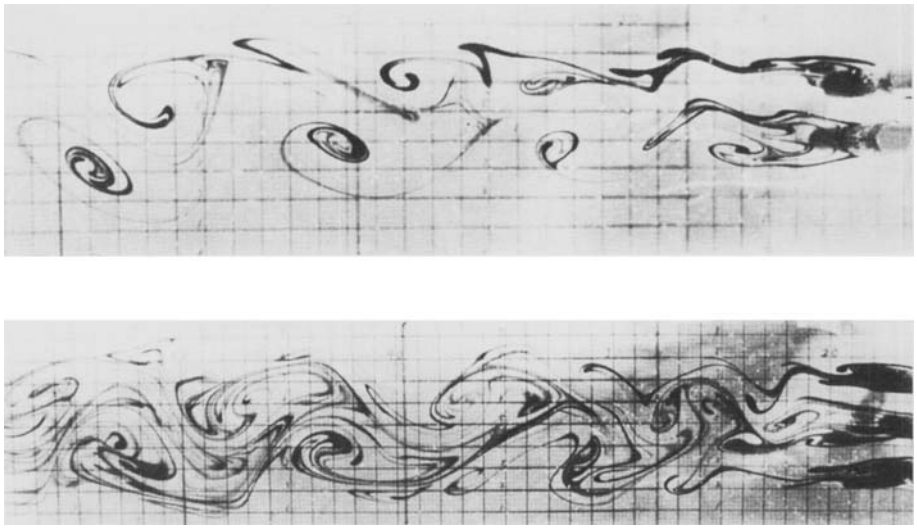

(a)

(b)

FIGURE 14. Asymmetric-flow regions. (a) Second harmonic mode of vortex shedding and deflected gap flow behind a pair of cylinders at an angle of stagger of 15°, $Re = 200$, $g^* = 1.0$. (b) Outward deflected gap flows behind three cylinders side by side, $Re = 200$, $g^* = 1.0$.

breaks down the gap flow generally remains biased and the doubled frequencies recommence after a few cycles. This type of intermittency is similarly reported for pairing of vortices in a mixing layer by Winant & Browand (1974).

In figure 12 the second mode is also shown to occur behind two flat plates side by side in steady flow. The gap flow is deflected downwards, and the higher frequency of vortex shedding occurs on the lower side of the wake. The range of gaps for which the asymmetric-flow regime is found for two flat plates is $g^* < 1.5$, and within this range the second harmonic mode is observed for $g^* = 0.6$–1.0. Rough measurements are made of the vortex-shedding frequencies from the outer edges of the two plates. Two people simply counted large numbers of shed vortices on both sides of the wake simultaneously, in measured times. Our frequency measurements of Strouhal frequency S are shown in figure 13. Down to $g^* = 1.3$ the shedding frequency on both plates is roughly that found for a flat plate in isolation at the same Re (200). In the range $1.0 < g^* < 1.3$ there is a good deal of scatter in the frequencies because no predominant shedding mode emerged. In the range $g^* = 0.6$–1.0 the higher frequencies were found to lie close to a line marking double the lower frequency, which corresponds with the second harmonic mode. Below $g^* = 0.6$ the wake approaches that associated with a plate the size of a two-plate combination.

The observations above described behind a pair of cylinders normal to a stream demonstrate flow phenomena which may be relevant to other cylinder configurations. For example we investigate briefly the case of two cylinders at an angle of stagger to the flow direction and the case of three cylinders side by side in an asymmetric-flow regime. The second harmonic mode is found to occur predominantly behind two cylinders for staggers up to about 15°,† as shown in figure 14 (a). With greater angles of stagger the vortices from the downstream cylinder dominate the wake and these vortices form the basis of a downstream large-scale Kármán street.

† The stagger angle is defined here as the angle between the line joining cylinder centres and a line perpendicular to the flow direction.

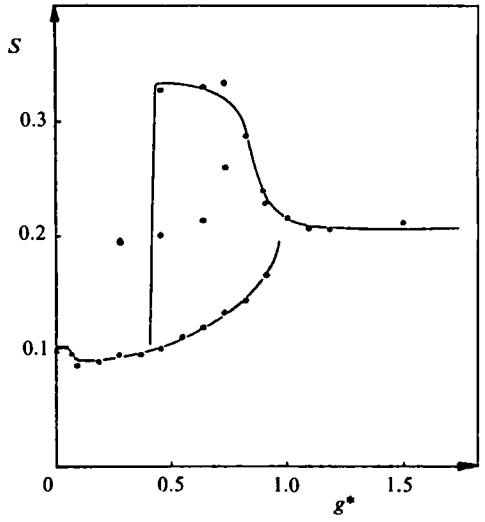

FIGURE 15. Hot-wire frequency measurements behind two circular cylinders side by side in a stream, from Spivack (1946).

In the case of three cylinders side by side, higher vortex-shedding frequencies are found for the outer two cylinders than for the central cylinder as the gap flows are deflected outwards, as demonstrated in figure 14(*b*). A large recirculating region behind the central cylinder sheds vortices at a low frequency, which then form the basis of a large-scale street downstream. The three-cylinder case thus exhibits a similar flow regime to the two-cylinder case.

4.3. *Discussion of the harmonic modes of vortex shedding*

The present visual observations of the vortex shedding in the near-wake region of the cylinders leads to a new interpretation of the many hot-wire measurements previously carried out behind two cylinders. Vortex-frequency measurements are typified by the results of Spivack (1946). His results are reproduced here in figure 15 showing his curves drawn through the data. Similar curves have been drawn through frequency data collected since (Ishigai *et al.* 1972; Bearman & Wadcock 1973; Quadflieg 1977; Kiya *et al.* 1980; Kamemoto 1976). In figure 16 we reinterpret the frequency data in terms of our observed harmonic vortex-shedding modes. All the data from the above investigations (for Reynolds numbers ranging from 10^3 to 4×10^4) have been plotted on a single graph, and the lower curve marked S_F is assumed to be the fundamental frequency. Dashed curves of twice and three times S_F are drawn above, and most of the data lie broadly along these curves. It is therefore probable that the frequency measurements at these higher Reynolds numbers also reflect the existence of the harmonic modes of vortex shedding that we have visualized in the present study.

The visualization in the present paper of the outward-deflected gap flows in the case of three cylinders side by side leads to higher frequencies and thinner wakes for the two outer cylinders compared with the central one. Judging from the two-cylinder case this suggests that the outer cylinders will experience a greater drag force than the inner central cylinder in the asymmetric-flow regime. Some drag-force measurements by Gerhardt & Kramer (1981) for a three-cylinder row at $Re = 10^7$ demonstrates that this is indeed the case.

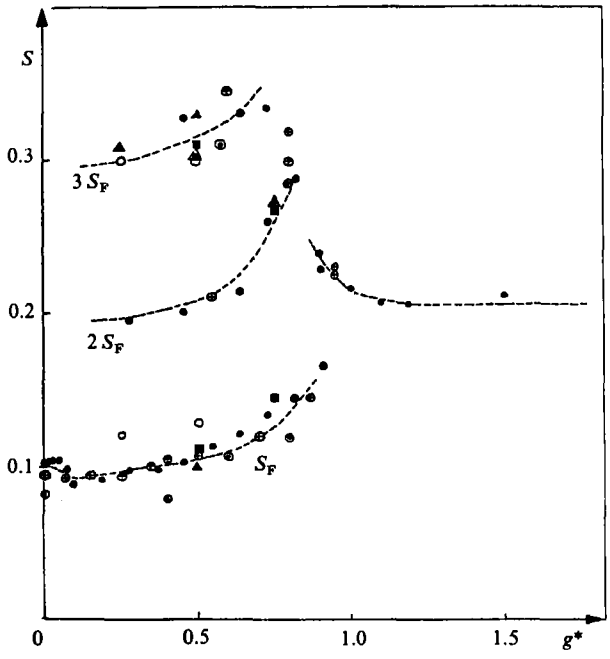

FIGURE 16. Hot-wire frequency measurements from other studies. The value S_F is the curve of fundamental frequency. The data lie broadly along curves marking twice and three times this frequency. ●, Spivack, $Re = 2.8 \times 10^4$; ○, Ishigai, 10^3–10^4; ⊕, Bearman & Wadcock, 2.5×10^4; ▲, Quadflieg, 3×10^4; △, Quadflieg (oscillating cylinders), 4×10^4; ⊙, Kiya *et al.*, 2×10^4; ■, Kamemoto, 3×10^4.

One question arises from the present visualization study: why does the gap flow become stably biased? Ishigai *et al.* and Quadflieg both described the phenomenon as a Coanda effect. However, our visualization shows that the gap flow is deflected behind two flat plates as well as behind two cylinders. Therefore a Coanda effect for two cylinders may be incidental but it does not cause the deflection. Some form of theoretical equilibrium or stability analysis on this problem may be profitable. We have shown the existence at low Reynolds numbers of two vortex pairs which are of distinctly unequal dimensions and cause an associated gap-flow deflection. Thus a first approach may be to consider theoretically such vortex-pair configurations behind two cylinders.

5. Conclusions

The use of flow-visualization methods in the present paper throws light on the mechanism by which the wakes of a pair of side-by-side bodies interfere with one another. In particular we observe how the wakes of multiple bodies can amalgamate to form single large-scale wakes.

It has previously been assumed that where the gaps between cylinders are such as to produce vortex-shedding synchronization ($g^* = 1.0$–5.0) then the resulting wake configuration will be either two parallel streets in phase, or two parallel streets in antiphase. The present paper shows that, following antiphase vortex shedding at the cylinders, the downstream wake is indeed two parallel streets in antiphase. This result agrees with previous work. The two antiphase streets are experimentally 'stable' in

that the configuration of vortices keeps its form for large distances downstream. However, in the case of in-phase vortex shedding, the configuration of two in-phase parallel streets does not occur except for a small region behind the cylinders. This idealized configuration is not experimentally 'stable' in the sense described above. We find that the wakes from each cylinder combine to form a single large-scale wake, defined here as a binary-vortex street. This combined wake is similar to a Kármán street except that, instead of the street being composed of single vortices, we have binary vortices which are pairs of like-signed vortices rotating round one another.

It is shown in the present paper that, even for smaller gaps when the flow is distinctly asymmetric, there are certain modes of vortex shedding. We find from flow visualization the existence of harmonic vortex-shedding modes behind pairs of cylinders (and also behind pairs of plates) at a Reynolds number of around 200. A new interpretation of hot-wire frequency measurements from other studies, based on the harmonic modes, suggests the existence of such modes of shedding at higher Reynolds numbers.

The experimental work described in this paper is mainly qualitative and it is hoped that the results will stimulate theoretical and numerical studies of such flows, as well as help to understand the vortex dynamics behind bluff bodies.

The author gratefully acknowledges the financial support of the Science and Enginering Research Council C.A.S.E. award between the University of Cambridge and the National Maritime Institute during the period 1978–1981, and the National Maritime Institute during the year 1981–1982. The author thanks in particular Professor J. E. Ffowcs Williams, his academic Supervisor at Cambridge University, and also Dr P. W. Bearman for helpful discussions. Funding for the colour plate is provided by the National Maritime Institute and particular thanks are due to Dr M. E. Davies for this.

REFERENCES

BEARMAN, P. W. & WADCOCK, A. J. 1973 The interaction between a pair of circular cylinders normal to a stream. *J. Fluid Mech.* **61**, 499–511.

BIERRMAN, D. & HERRNSTEIN, W. H. 1933 The interference between struts in various combinations. *NACA TR* 468.

CIMBALA, J. M. 1984 Large structure in the far wakes of two-dimensional bluff bodies. Ph.D. thesis, California Institute of Technology.

GERHARDT, H. J. & KRAMER, C. 1981 Interference effects for groups of stacks. *J. Wind Engng & Ind. Aero.* **8**, 195–202.

ISHIGAI, S., NISHIKAWA, X., NISHIMURA, X. & CHO, X. 1972 Experimental study on structure of gas flow in tube banks with axis normal to the flow. *Bull. JSME* **15**, 949–956.

KAMEMOTO, K. 1976 Formation and interaction of two parallel vortex streets. *Bull. JSME* **19**, 283–290.

KIYA, M., ARIE, M., TAMURA, H. & MORE, H. 1980 Vortex shedding from two circular cylinders in staggered arrangement. *Trans. ASME* **102**, 166–173.

LAMB, H. 1932 *Hydrodynamics*, pp. 221–223. Cambridge University Press.

LANDWEBER, L. 1942 Flow about a pair of adjacent parallel cylinders normal to a stream. *David Taylor Mod. B. Rep.* 485, Washington.

PRESTON, J. & SWEETING, N. E. 1943 An improved smoke generator for use at high Reynolds numbers. *ARC R & M* 2023.

QUADFLIEG, H. 1977 Vortex induced load on the cylinder pair at high *Re*. *Forsch. Ing. Wes.* **43**, 9–18.

ROBERTS, B. W. 1962 Aeroelastic vibrations in a row of circular cylinders. Ph.D. thesis, Cambridge University.

SPIVACK, H. M. 1946 Vortex frequency and flow pattern in the wake of two parallel cylinders at varied spacings normal to an airstream. *J. Aero. Sci.* **13**, 289–297.

THOMAS, O. G. & KRAUS, K. A. 1964 Interaction of vortex streets. *J. Appl. Phys.* **35**, 3458–9.

WINANT, C. D. & BROWAND, F. K. 1974 Vortex pairing, the mechanism of turbulent mixing layer growth at moderate Reynolds number. *J. Fluid Mech.* **63**, 237–255.

ZDRAVKOVICH, M. 1968 Smoke observations of the wake of a group of three cylinders at low Reynolds number. *J. Fluid Mech.* **32**, 339–351.

ZDRAVKOVICH, M. 1977*a* Review of flow interference between two circular cylinders in various arrangements. *Trans. ASME* I: *J. Fluids Engng* 618–633.

ZDRAVKOVICH, M. 1977*b* Interference between two circular cylinders; series of unexpected discontinuities. *J. Ind. Aero.* **2**, 255–270.